Super Ultrawideband Planar Inverted F Antenna on Paper based Substrate with Low SAR

Sakshi Kumari[1†] and **Vibha Rani Gupta**[2], Non-members

ABSTRACT

In this paper, a super ultrawide band planar inverted F antenna (PIFA) has been proposed for wearable applications on a low cost, ecofriendly paper-based substrate. This work is a first and important step towards the progression of conformal flexible antennas for a body area network. The proposed antenna has measured impedance bandwidth of 10.6 GHz, which covers almost all the bands of a wireless body area network i.e. GSM (880–960 MHz), GPS (1565–1585 MHz), DCS (1710–1880 MHz), PCS (1850–1990 MHz), UMTS (1920–2170 MHz), ISM (2.4–2.4835 GHz), WiMAX (3.3–3.8 GHz), HiperLAN (5.15–5.35 GHz), WLAN (5.725–5.850 GHz) and UWB (3.1–10.6 GHz). Initially, the electrical characteristics of paper are extracted using Cavity Resonator and Transmission line method and then used for the design and fabrication of the proposed antenna. The measured results are in good agreement with the simulated results. This paper also focuses on analysis of the effect of electromagnetic absorption in terms of specific absorption rate for a human arm with frequency exposure at 0.9 GHz, 1.5 GHz, 1.8 GHz, 3.5 GHz, 2.45 GHz, 5.2 GHz and 5.8 GHz and is found to be within the recommended limit by FCC.

Keywords: Electromagnetic wave absorption, paper based substrate, specific absorption rate, ultrawideband antennas.

1. INTRODUCTION

In recent years, wireless body area networks (WBAN) has attracted incredible attention to the development of low profile, light weight, compact wearable antennas which enable them to communicate with each other on a human body [1]. The frequency bands used for Wireless Body Area Network applications are GSM, GPS, DCS, WiMAX, ISM, HiperLAN, WLAN, and UWB. Wearable antennas in WBAN are used with the transceiver to send and receive the information between the two devices or between doctors and patients and to send the location of the patient. In the past, few multiband antennas based on FR-4 substrate, which covers some of the above bands have been reported like GPS, PCS, WiMAX and UWB bands are covered in [2–3]. But as per the best knowledge of the author, no papers have been reported which cover all the above-mentioned bands for the wearable application based on flexible substrate with low SAR value.

Different flexible materials such as denim, textile, shieldIt, jute, wool have been explored for the design of wearable antennas [4–7]. Paper, being one of the least expensive, flexible, recyclable, biodegradable, ecofriendly organic materials, is extensively being researched as a substrate for wearable applications. Apart from the flexibility, it also provides low profile and low fabrication cost. The only drawback associated with paper as substrate is that it is hydrophilic in nature. Some of the antennas that have been reported on paper substrate are monopole patch antenna with wide frequency band, starting from 2 GHz up to over 10 GHz [8–9], U slot monopole antenna for GPS, WiMAX, HiperLAN/2, WLAN bands [10–12], Z shaped CPW fed monopole for GPS [13], PIFA for WLAN [14] and inkjet printed SIW antennas [15–16]. Paper has also been used for developing RFID UHF antennas for frequency range 902 to 920 MHz [17–18]. An antenna array (1 × 2 Patch) on paper substrate for 2.4 GHz [19] has also been reported. Most of the antennas reported are either for a particular application or of monopole configuration which have only partial ground plane.

The deployment of a wireless body area network induces biological and health effects which should be evaluated carefully. The electromagnetic exposure, which affects the health, is usually measured in terms of absorbed power. SAR has been analyzed using EM simulation tools with human phantom models for evaluating the interactions between the human body and antennas for WBAN.

As reported earlier monopole patch antenna has been used for wider bandwidth but has high SAR value due to the presence of a partial ground plane at the bottom side of the substrate, especially at lower frequencies [20]. Another disadvantage with the monopole antenna is that, its performance characteristics are detuned in the presence of a human body. The microstrip patch has advantages over these two limitations of monopole patch antenna due to the presence of a ground plane but has its own limitations of larger size and narrow bandwidth.

Manuscript received on June 17, 2019 ; revised on September 25, 2019 ; accepted on October 21, 2019.

The authors are with Department of Electronics and Communication Engineering, Birla Institute of Technology, Mesra, India. E-mail : sakshi501@gmail.com[1], vrgupta@bitmesra.ac.in[2]

†Corresponding author.

Planar inverted F antenna having a ground plane on the bottom side of the substrate, which helps in reducing SAR, is the best candidate for wearable applications. The conventional PIFA has narrow bandwidth which can be increased by stub, capacitive, inductive loading, utilizing meandered slotted ground plane [21], optimizing feed plate, shorting plate [22] and feedplate silhouettes [23].

In this paper, a planar inverted F antenna on paper substrate is designed and analyzed. Compared with traditional multiband PIFAs [24–26], the proposed PIFA covers more bands with an unmodified ground plane and provides low SAR value. The novelty of the proposed antenna is that it is designed on the flexible substrate and a single antenna can be used for voice communication, location, identification, communication between equipment and transfer of data to the doctors.

Sections 2 and 3 present material characterization and the geometry of the proposed antenna respectively. The design approach and the parametric studies carried out to decide the values of different parameters of antenna design are discussed in detail in Section 4. While Section 5 discusses the simulated and measured results and finally conclusions are presented in the last Section 6.

2. DIELECTRIC (RF) CHARACTERIZATION OF PAPER SUBSTRATE

There are wide varieties of paper available in the market which differ in density, texture and electromagnetic characteristics (dielectric constant and dielectric loss tangent). Therefore, electromagnetic characterization of paper substrate becomes a mandatory procedure prior to any antenna design on it. The paper used here as substrate is glossy coated drawing paper (coated one side, "C1S") which is usually thicker than writing paper. The thickness of each sheet of paper is around 0.216 mm. The glossy coated paper is taken to reduce the absorbency of atmospheric humidity to some extent. Six sheets of paper are stacked together to obtain a thickness of 1.3 mm. A copper laminate of 0.3 mm is pasted at the bottom side of the paper substrate to obtain the final thickness of 1.6 mm.

The dielectric characterization of paper has already been carried out by many researchers for microwave frequencies and the relative permittivity is found to be in a consistent range between 2.5 and 4. Various methods for characterization of paper such as use of T resonator [16], cavity perturbation method [27–28], ring resonator method [18, 29] and transmission line method [30–31] are reported in the literature. In the present report, paper substrate is characterized using two methods, namely cavity resonator and transmission line method.

2.1 Cavity Perturbation Method

The measurement system, for the cavity perturbation method, consists of vector network analyzer (VNA), and 85071E split post dielectric resonators (SPDR). The measurement of dielectric properties involves two steps. First, the resonant frequency and quality factor of an empty cavity are measured. In the second step, the measurement procedure is repeated with the cavity loaded with material under test. The permittivity of the material can then be calculated using the change in frequency, volume and Q-factor. The cylindrical shaped solid sample of paper is prepared and used for the test. The formulas used for the material characterization are as follows [32]. Real part of dielectric constant is:

$$\epsilon' = 1 + \frac{V_c(f_c - f_s)}{2V_s f_s} \tag{1}$$

and imaginary part of dielectric constant is:

$$\epsilon'' = \frac{V_c}{4V_s}\left(\frac{1}{Q_s} - \frac{1}{Q_c}\right) \tag{2}$$

where, f_c = resonant frequency of the empty cavity resonator, f_s = resonant frequency of the resonator loaded with material under test, Q_c = Q-factor of empty cavity resonator, Q_s = Q-factor of cavity loaded with material under test, V_c = volume of empty cylindrical resonator and V_s = volume of material under test inside the cavity resonator.

The measured values are: $\epsilon'_r = 2.82$, $\epsilon''_r = 0.0987$, dielectric constant = 2.82 and loss tangent = 0.035.

2.2 Transmission Line Method

In this method, two 50 Ω microstrip lines of length 100 mm and 50 mm of 4 mm width each are fabricated on the paper substrate whose dielectric constant is to be measured. The effective relative permittivity is obtained using the following formula [30]:

$$\epsilon_{reff} = \left[\frac{\Delta\theta \times c}{2\pi f(\Delta L)}\right]^2 \tag{3}$$

where, $\Delta\theta$ is the phase difference between the scattering parameters of the two transmission lines, ΔL is

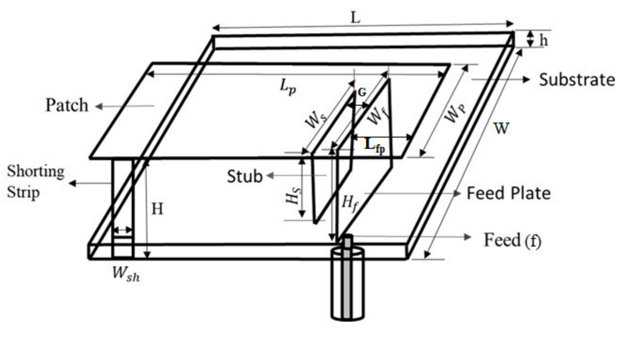

Fig.1: *Proposed antenna geometry.*

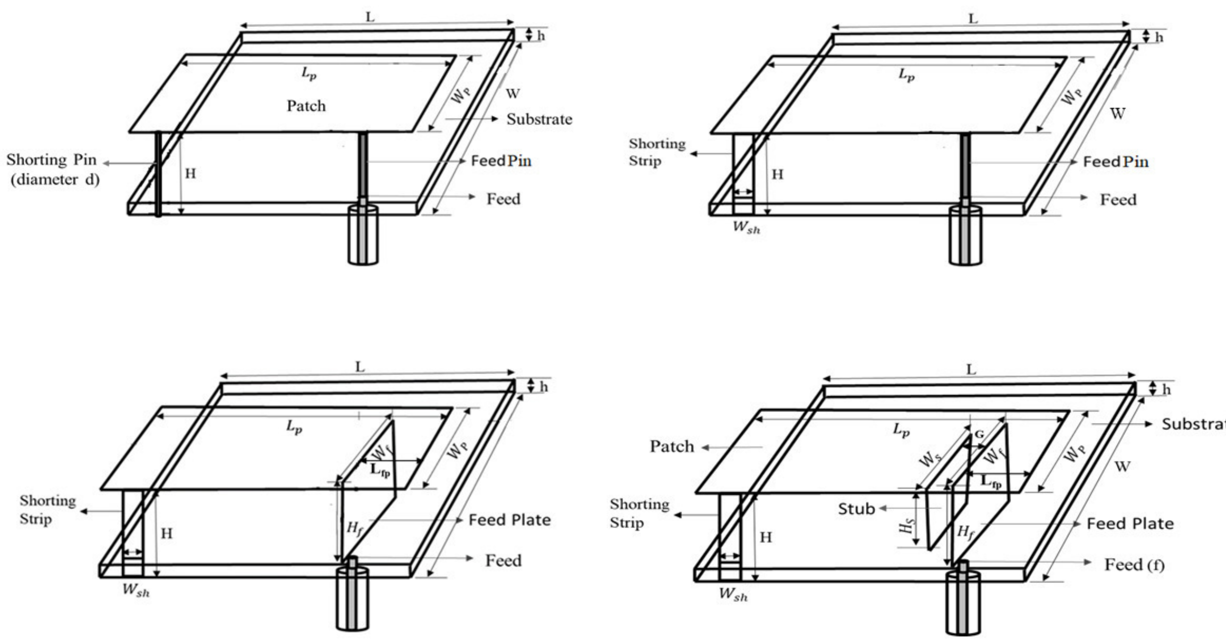

Fig.2: Design approach of proposed antenna.

Table 1: Detailed optimized dimensions of PIFA.

Antenna Parameters	Dimension (mm)
Substrate ($L \times W \times h$)	$60 \times 40 \times 1.6$
Ground plane ($L \times W \times t$)	$60 \times 40 \times 0.3$
Patch ($L_P \times W_P \times t$)	$60 \times 40 \times 0.3$
Feed plate width (W_f)	30
Feed plate height (H_f)	6.3
Shorting plate width (W_{sh})	5
Shorting plate height (H)	7.9
Stub width (W_S)	30
Stub height (H_S)	5.75

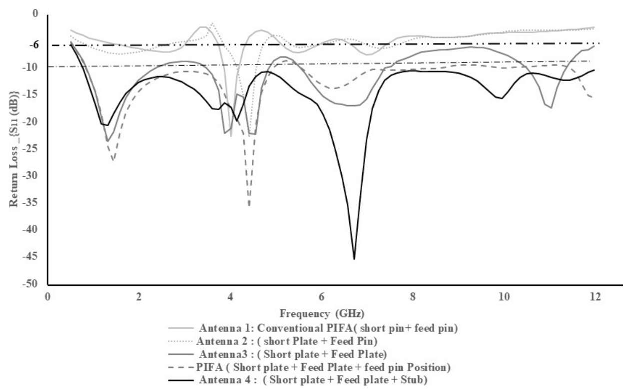

Fig.3: Simulated reflection coefficient of designed PIFA.

the difference in length between the two transmission lines, c is the speed of light and f is the frequency. Thus, the relative permittivity of the material is given as:

$$\epsilon_r = \frac{2\epsilon_{reff} - 1 + x}{1 + x} \tag{4}$$

where x is given as

$$x = \left(1 + \frac{12h}{w}\right)^{-0.5} \tag{5}$$

Loss tangent is calculated using formula [31]

$$tan\delta = \frac{\alpha_d \lambda_0 \sqrt{\epsilon_{reff}}(\epsilon_r - 1)}{\pi \epsilon_r (\epsilon_{reff} - 1)} \tag{6}$$

where, α_d is attenuation constant, λ_0 is wavelength in free space, ϵ_{reff} is effective relative permittivity and ϵ_r is relative permittivity. The relative permittivity (ϵ_r), calculated over the frequency range 0.5 to 12 GHz lies in the range of 2.8 to 2.82 while loss tangent is 0.0349.

3. GEOMETRY OF PROPOSED ANTENNA

The configuration of the proposed planar inverted F antenna is illustrated in Fig. 1. The radiating patch has dimension of $L_P \times W_P \times t$ mounted on the substrate with dimensions $L \times W \times h$ at the height H. The space between the top radiating patch and substrate is filled with air (free space). The dimensions of the feed plate are $W_f \times H_f \times t$. Another rectangular metallic plate with dimensions $W_S \times H_S \times t$ is placed parallel to the feed plate above the substrate. This plate works as a stub for the impedance matching. The antenna is shorted to the ground with the help of a rectangular plate of size $W_{sh} \times H \times t$.

High Frequency Simulation Software (HFSS) is used to optimize the design of the proposed antenna.

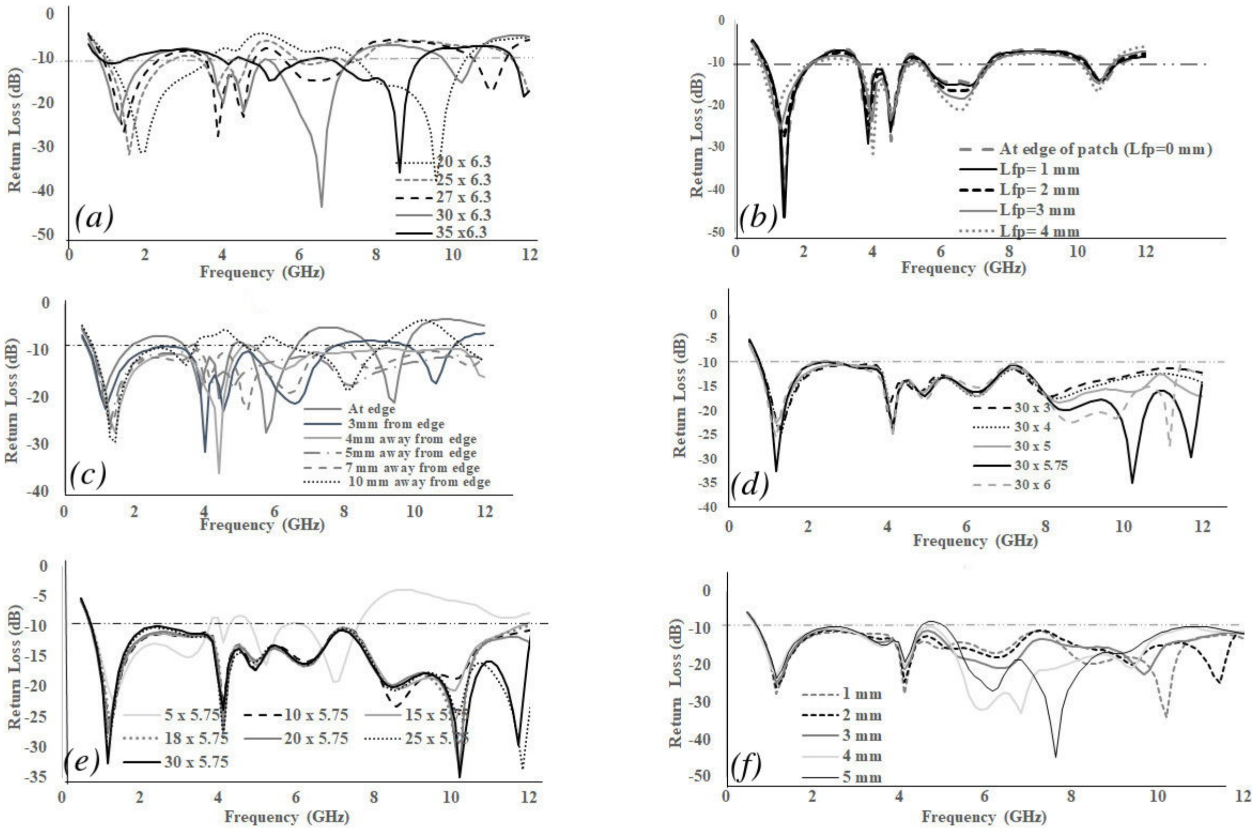

Fig.4: *Simulated reflection coefficient response for (a) feedplate width (W_f) variation at constant height of 6.3 mm, (b) position of feedplate varied with respect to patch width (W_P), (c) feed pin position variation along the edge of feed plate's width (W_f) with respect to feedplate's height (H_f), (d) stub height (H_S) variation, (e) stub width (W_S) variation keeping stub height fixed, and (f) distance between stub and feedplate (G) variation.*

Based on the parametric analysis, which is discussed in the next section, the detailed optimized dimensions are listed in Table 1.

4. DESIGN APPROACH AND PARAMETRIC STUDIES

The steps followed to reach the final structure are discussed in this section. Fig. 2 shows the design approach of the proposed antenna while its optimized simulated return loss (S_{11}) plots are depicted in Fig. 3.

The design approach starts with the design of conventional PIFA (Antenna 1) on paper-based substrate. A radiating patch of dimension $L_P \times W_P$ is mounted at the top of the substrate ($L \times W$) with ground plane maintained on the opposite side. The radiating patch is fed using a 50-Ω coaxial probe and shorted at the edge by a shorting pin of diameter "d".

The design equations used for planar inverted F antenna are as follows:

$$L_p + W_p - W_{sh} = \frac{\lambda_0}{4} \tag{7}$$

$$\lambda_0 = \frac{c}{f_r\sqrt{\epsilon_r}} \tag{8}$$

where, λ_0 is the operating wavelength, c is the speed of light, equal to 3×10^8 m/s, and ϵ_r is the relative permittivity.

Initially, the dimension of the conventional PIFA (Antenna 1) are calculated using the above formula and considering the central frequency. But the simulated result shows a narrow bandwidth at frequency 4.01 GHz with reference to $S_{11} < -10$ dB. Next, the short pin is replaced by the shorting strip (Antenna 2). The width of the shorting strip is analyzed by parametric analysis and the best improvement is observed at 5 mm, but it helps only in shifting the frequency towards the higher frequency range. No improvement in bandwidth is observed. So, to improve the bandwidth, the feed pin is replaced by a feed plate and the design parameters are modified (Antenna 3). The dimensions of the feed plate are $W_f \times H_f \times t$, where t is the thickness of copper. The width of the feedplate is decided through parametric analysis as shown in Fig. 4(a). The optimized dimensions of the feedplate are $30\times6.3\times7.9\ mm^3$. Also, the optimization is done to decide the position of the feed

Table 2: *Simulated and measured gain of proposed antenna in free space for GSM, GPS, DCS, ISM, WIMAX and HiperLAN bands.*

Frequency Band	GSM	GPS	DCS	ISM	WiMAX	WLAN	HiperLAN
Center Frequency (GHz)	0.9	1.5	1.8	2.45	3.5	5.2	5.8
Simulated Gain (dB)	0.98	0.99	1.66	5.05	6.95	7.71	7.66
Measured Gain (dB)	0.99	1.20	1.98	5.2	6.45	7.6	7.5

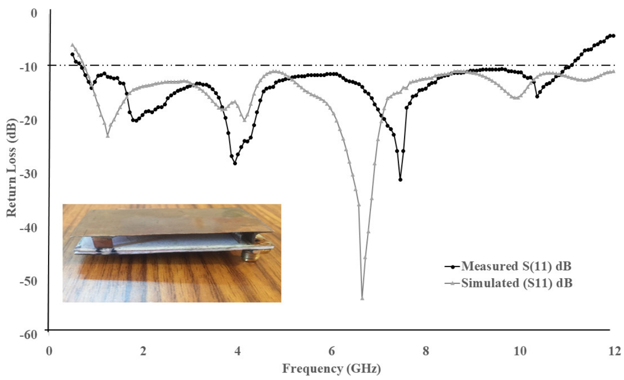

(a)

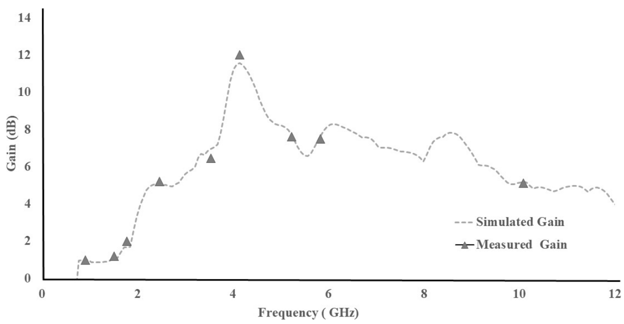

(b)

Fig.5: *Simulated and measured (a) reflection coefficient (S_{11}) and (b) gain of proposed antenna.*

plate with respect to the radiating patch's width i.e. the distance between the feedplate and the edge of the patch's width, denoted by L_{fp} (Antenna 3). Its simulated return loss (S_{11}) versus frequency curves for different values of L_{fp} are depicted in Fig. 4(b). Next, the parametric study is done to optimize the feed pin position along the edge of the feedplate's width (W_f) and with respect to H_f, illustrated in Fig. 4(c). Return loss characteristics of Antenna 3 in Fig. 3 with the optimized dimensions of the feedplate ($30 \times 6.3\ mm^2$) and feed position (3 mm away from the edge of the feedplate's width along W_f) shows the improvement in impedance bandwidth. It covers the frequency range 0.63 GHz to 11.9 GHz with reference to $S_{11} < -6$ dB. To further improve the impedance matching, a metallic plate of rectangular dimension ($W_S \times H_S \times t$) is placed at a distance of 'G' from the feedplate (Antenna 4) which acts as a stub to improve mismatch. This is the final proposed antenna. The dimensions of the stub are decided by parametric studies. The width of the stub is kept constant (30 mm) and its height is varied from 3 mm to 6 mm, shown in Fig. 4(d) and the best result is obtained at the stub size of 30 mm × 5.75 mm. After deciding the height of the stub i.e. 5.75 mm, the width of the stub is varied from 5 mm to 35 mm to verify the result at other dimensions, illustrated in Fig. 4(e). Thus, the results are best at stub width of 30 mm. To improve the impedance matching at desired frequencies, the separation distance between feedplate and stub is also studied between 1 mm to 5 mm, shown in Fig. 4(f). The optimized distance between stub and feedplate is 1 mm. With the optimized dimensions, which are tabulated in Table 1, the simulated return loss of Antenna 4 (Fig. 3) shows that it covers the frequency range from 0.77 GHz to beyond 12 GHz with reference to –10 dB and covers all the required applications of BAN.

5. RESULT AND DISCUSSIONS

The various performance characteristics of PIFA in free space and in the vicinity of human body parts are investigated below.

5.1 Performance in free space

Fig. 5 shows the prototype of the proposed antenna for BAN. The performance characteristics of the developed antenna are measured and compared in Fig. 5 and Fig. 6. The comparison of simulated and measured S_{11} parameters is shown in Fig. 5(a). The graph shows that the designed antenna has measured bandwidth of 10.6 GHz, covering frequency range from 0.7 GHz to 11.3 GHz, which includes all the necessary bands (GSM, GPS, DCS, PCS, UMTS, ISM, WiMAX, HiperLAN, WLAN and UWB), which may be required for the Body Area Network. The feedplate and the stub has been successfully utilized to obtain the desired bandwidth. There is slight variation in the measured and simulated results due to fabrication and measurement errors. The simulated and measured gain of the proposed antenna shown in Fig. 5(b) depicts that the gain lies in the range of 0.98 dB to 11.55 dB over the desired frequency band. The maximum simulated gain is 11.55 dB at 4.15 GHz, while the maximum measured gain obtained at the same frequency is 12 dB. The gain is varying from 0.98 dB to 1.98 dB for lower frequency bands. This is due to the fact that the loss is more at lower frequency. The simulated and measured gain at

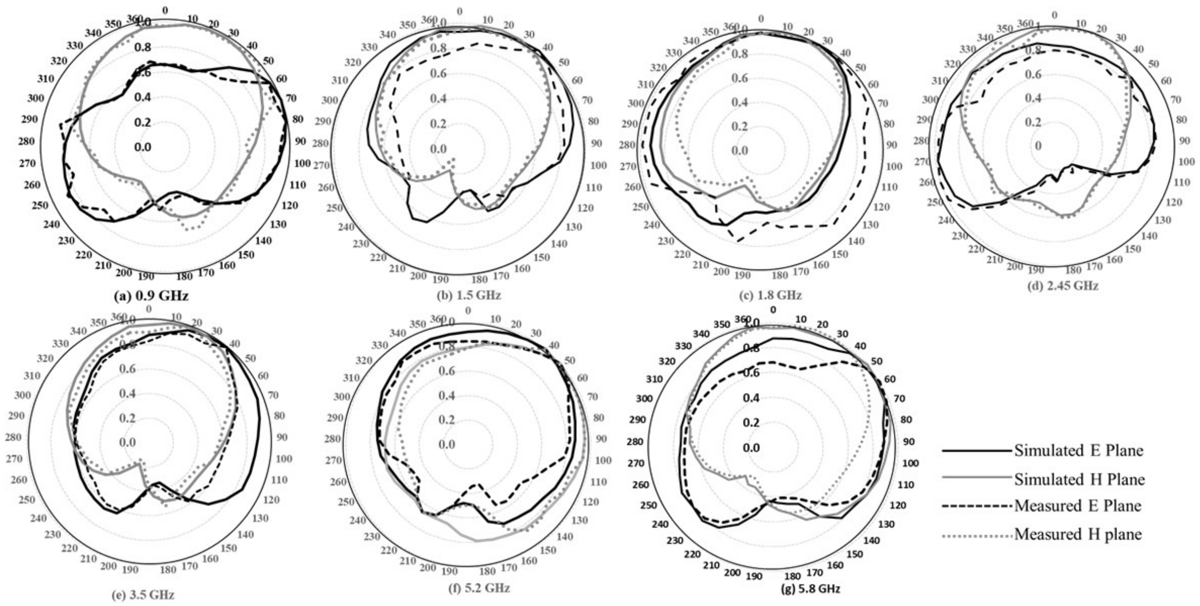

Fig. 6: *Normalized E plane and H plane radiation pattern of proposed antenna in free space for (a) GSM, (b) GPS, (c) DCS, (d) ISM, (e) WIMAX and (f) HiperLAN bands.*

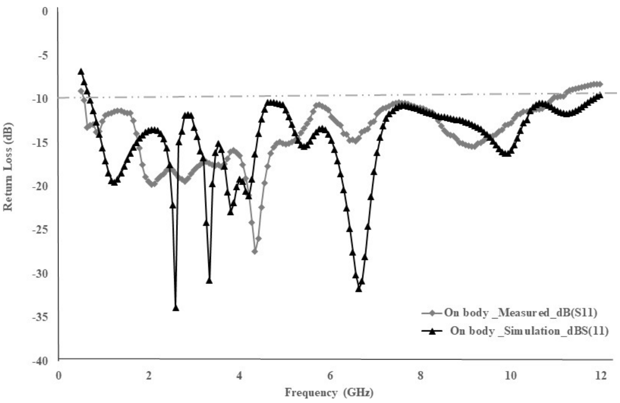

Fig. 7: *Simulated and measured reflection coefficient of proposed antenna on human arm.*

desired frequency bands are shown in Table 2. The E plane and H plane radiation patterns at several important frequencies are depicted in Fig 6. It is evident from the figure that all the radiation patterns exhibit almost omnidirectional characteristic at all the frequencies.

5.2 Antenna Performance in the Presence of a Human Body and SAR

The interaction of the antenna with the body parts depends on the electrical properties of body tissues at different frequencies. Hence the electrical properties of biological tissues are also characterized at different frequencies. For evaluating antenna performance and measuring SAR, a human arm is modelled in HFSS [20], considering the biological tissue's conductivity, permittivity and loss tangent at 0.9 GHz, 1.5 GHz, 1.8 GHz, 2.45 GHz, 3.5 GHz, 5.2 GHz and 5.8 GHz [33]. The simulated and measured reflection coefficient (S_{11}) of planar inverted F antenna when placed on a human arm is shown in Fig. 7. The simulated bandwidth is 11.07 GHz covering frequency range 0.7 GHz to 11.77 GHz, while the measured bandwidth is 10.33 GHz covering frequency range 0.57 GHz to 10.90 GHz, still covering the desired bands. There is not much variation in the bandwidth of the designed antenna due to the presence of the ground plane of PIFA. A little shift is observed when placed on the human arm, but it still covers all the frequency bands of the desired applications.

Fig. 8 depicts the plot of specific absorption rate (SAR) field distribution for desired frequencies. The recommended limit of the SAR by FCC is 4 Watt/kg for human arm/forearm [34]. The simulated peak SAR of the proposed antenna lies in the range of 0.03 Watt/kg to 0.69 Watt/kg. The method proposed in [20] is used to measure the SAR of the proposed antenna in useful bands. The simulated peak SAR values and measured SAR compared with simulated values are shown in Fig. 9 and Fig. 10 respectively which matches quite reasonably. There is slight discrepancy in the measured and simulated SAR values due to actual dielectric characterization of body tissues and measurement tolerence. Hence the proposed antenna can be safely used for the BANs.

5.3 Group Delay

Group delay is an important parameter of performance characteristic for an UWB antenna [35]. Two identical proposed Planar Inverted F Antennas are placed in the far field region of each other which is

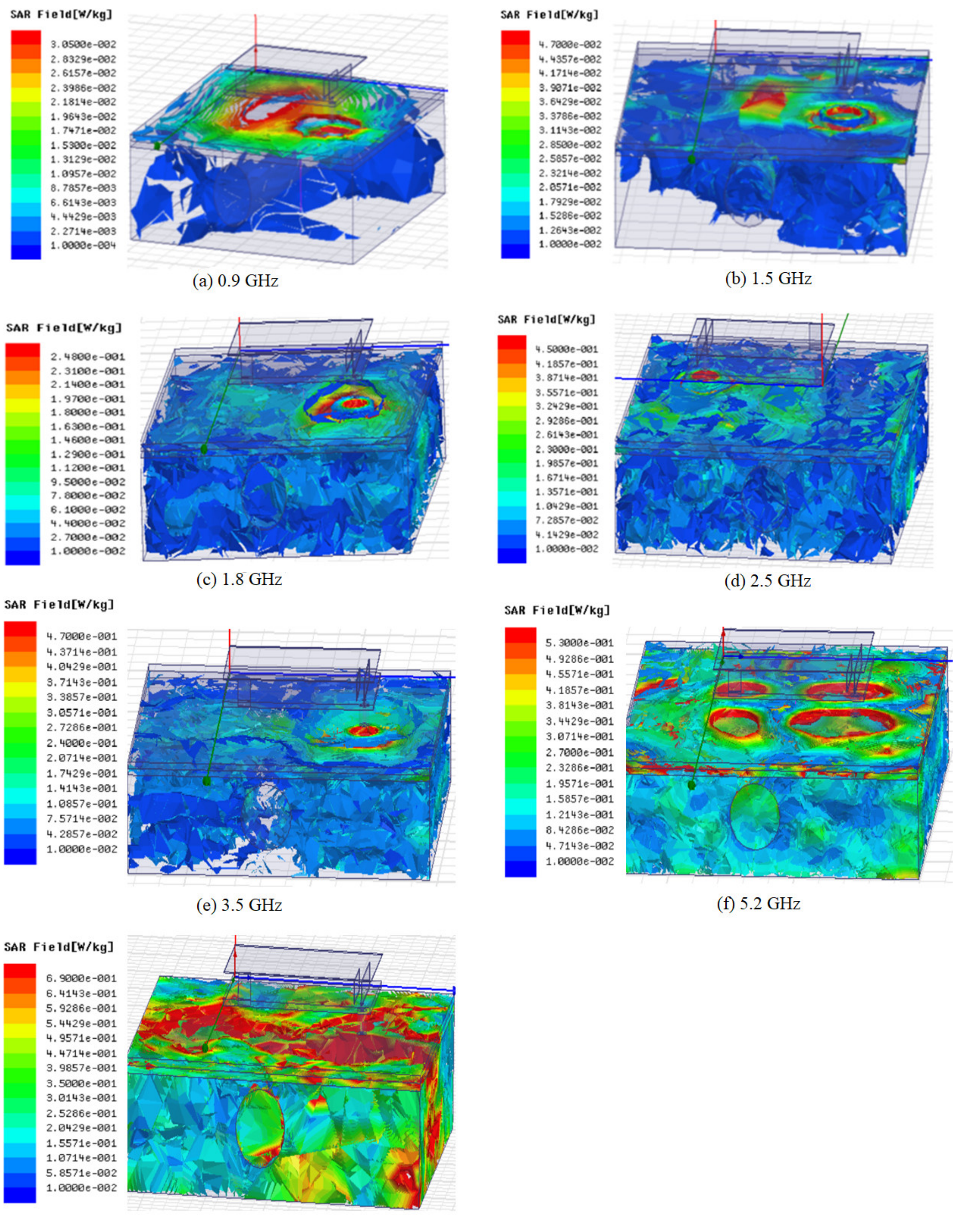

(a) 0.9 GHz

(b) 1.5 GHz

(c) 1.8 GHz

(d) 2.5 GHz

(e) 3.5 GHz

(f) 5.2 GHz

(g) 5.8 GHz

Fig.8: *Simulated SAR field distribution in a human arm at exposure of centre frequencies of desired bands.*

greater than $2D^2/\lambda$ (D is the maximum dimension of antenna and λ is wavelength) in front to front orientation. The simulated group delay response in Fig. 11 depicts that the designed antenna provides a time-domain response without considerable distortion. Two scenarios have been considered for measurement of group delay. In the first case, both the transmitting antenna and the receiving antenna are placed off body. The group delay varies from 0.16 ns to 0.66 ns at desired bands of application with maxi-

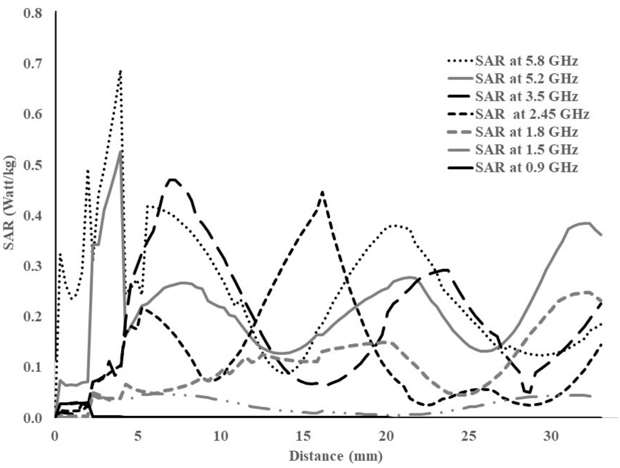

Fig.9: *Peak SAR plot at different frequencies.*

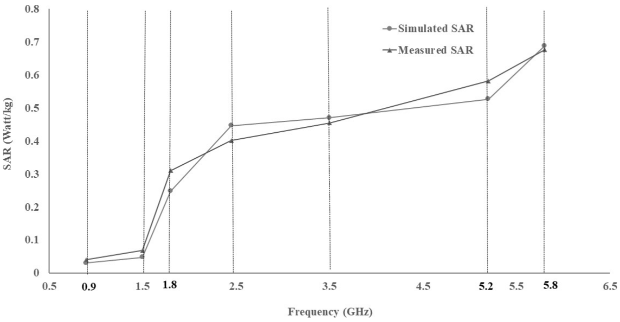

Fig.10: *Comparison of simulated and measured SAR for human arm at desired frequencies.*

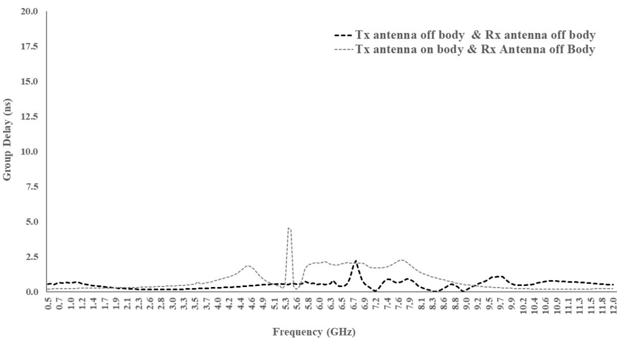

Fig.11: *Simulated group delay response.*

mum delay of 2.2 ns at 6.77 GHz. While in the second case when the transmitting antenna is placed on a human arm and the receiving antenna is placed off body in the far field region, the group delay varies in the range of 0.23 ns to 1.96 ns at desired bands of application with maximum delay of 4.54 ns at 5.39 GHz. Thus, the proposed antenna exhibits good phase linearity with small variation in group delay response in the entire frequency band.

6. CONCLUSION

In this paper, a super ultra wideband Planar Inverted F Antenna covering the frequency range 0.7 GHz to 11.3 GHz with an impedance bandwidth of 10.6 GHz ($S_{11} < -10$ dB) and gain ranging from 0.96 dB to 11.55 dB has been proposed. One of the least expensive, flexible and ecofriendly substrates i.e. a paper has been considered for the design of antenna. A single antenna covers all the frequency bands required for the BANs (GSM (880–960 MHz), GPS (1565–1585 MHz), DCS (1710–1880 MHz), PCS (1850–1990 MHz), UMTS (1920–2170 MHz), ISM (2.4–2.48 GHz), WiMAX (3.3–3.8 GHz), HiperLAN/2 (5.15–5.35 GHz), WLAN (5.725–5.85 GHz) and UWB band (3.1–10.6 GHz)). The peak SAR is 0.69 Watt/kg which is quite below the public safety RF exposure limit of 4 Watt/kg, specified by the FCC.

References

[1] R. Negraa, I. Jemilia and A. Belghith, "Wireless Body Area Networks: Applications and technologies," *Procedia Computer Science*, vol. 83, pp. 1274-1281, 2016.

[2] I. Zahraoui, A. Errkik, J. Zbitou, E. Abdelmounim, L.E. Abdellaoui and A. Mediavilla, "New Low Cost Printed Antenna CPW-Fed for Global Positioning System, Personal Communication System and Worldwide Interoperability for Microwave Access Band Applications," *International Journal of Engineering Transaction B: Applications*, vol. 29, no. 8, pp. 1056-1061, 2016.

[3] I. J. G. Zuazola and J. C. Batchelor, "Compact Multiband PIFA type Antenna," *Electronics Letter*, vol. 45, 2009.

[4] P. J. Soh, G. A. E. Vandenbosch, S. L. Ooi and N. M. Rais, "Design of a Broadband All Textile Slotted PIFA," *IEEE Transactions on Antennas and Propagation*, vol. 60, no. 1, pp. 379-384, 2012.

[5] I. Gil and R. F. GarcÃŋa, "Wearable PIFA antenna implemented on jean substrate for wireless body area network," *Journal of Electromagnetic Waves and Applications*, pp. 1-11, 2017.

[6] M. I. Ahmed, M. F. Ahmed, A. A. Shaalan, "Investigation and Comparison of 2.4 GHz Wearable Antennas on Three Textile Substrates and Its Performance Characteristics," *Open Journal of Antennas and Propagation*, vol. 5, pp. 110-120, 2017.

[7] K. Zeouga, L. Osman, A. Gharsallah, B. Gupta, "Truncated Patch Antenna on Jute Textile for Wireless Power Transmission at 2.45 GHz," *International Journal of Advanced Computer Science and Applications*, vol. 9, no. 1, pp. 301-305, 2018.

[8] G. Shaker, S. S. Naeini, N. Sangary, and M. M. Tentzeris, "Inkjet Printing of Ultrawideband

(UWB) Antennas on Paper-Based Substrates," *IEEE Antennas and Wireless Propagation Letters*, vol. 10, pp. 111-114, 2011.

[9] H. P. Phan, T. P. Vuong, P. Benech, P. Xavier, P. Borel and A. Delattre, "Low-Cost Wideband Antenna on Paper Substrate," in *11th IEEE European Conference on Antennas and Propagation (EUCAP)*, 2017.

[10] H. F. Abutarboush and A. Shamim, "Paper-Based Inkjet-Printed Tri-Band U-Slot Monopole Antenna for Wireless Applications," *IEEE Antennas and Wireless Propagation Letters*, vol. 11, pp. 1234-1237, 2012.

[11] W. N. N. W. Marzudi, Z. Z. Abidin, S. H. Dahlan, K. N. Ramli and M. R. Kamarudin, "Performance of star patch antenna on a paper substrate material," *ARPN Journal of Engineering and Applied Sciences*, vol. 10, no. 19, pp. 8606-8612, 2015.

[12] D. S. Marotkar and P. L. Z. Yeshwantrao, "Microstrip Antenna with Photographic Paper Substrate for WLAN," *International Journal of Informatics and Communication Technology*, vol. 7, no. 2, pp. 67-70. 2018.

[13] A. M. Mansour, N. Shehata, B. M. Hamza and M. R. M. Rizk, "Efficient Design of Flexible and Low-Cost Paper-Based Inkjet-Printed Antenna," *International Journal of Antennas and Propagation*, pp. 1-6, 2015.

[14] D. E. Anagnostou, A. A. Gheethan, A. K. Amert and K.W.Whites, "A Direct-Write Printed Antenna on Paper-Based Organic Substrate for Flexible Displays and WLAN Applications," *Journal of Display Technology*, vol. 6, no. 11, pp. 558-564, 2010.

[15] R. Moro, M. Bozzi, S. Kim and M. Tentzeris, "Novel Inkjet-Printed Substrate Integrated Waveguide (SIW) Structures on Low-Cost Materials for Wearable Applications," in *Proc. of the 42nd European Microwave Conference*, Netherlands, 2012.

[16] S. Kim, B. Cook, T. Le, J. Cooper, H. Lee, V. Lakafosis, R. Vyas, R. Moro, M. Bozzi, A. Georgiadis, A. Collado and M.M. Tentzeris, "Inkjet-printed antennas, sensors and circuits on paper substrate," *IET Microwave and Antenna Propagation*, vol. 7, no. 10, pp. 858-868, 2013.

[17] S. Kim, A. Georgiadis and M. M. Tentzeris, "Design of Inkjet-Printed RFID-Based Sensor on Paper: Single and Dual-Tag Sensor Topologies," *Sensors*, vol. 18, no. 1958, 2018.

[18] A. Rida, L. Yang, R. Vyas and M.M. Tentzeris, "Conductive Inkjet-Printed Antennas on Flexible Low-Cost Paper-Based Substrates for RFID and WSN Applications," *IEEE Antennas and Propagation Magazine*, vol. 51, no. 3, pp. 13-23, 2009.

[19] F. Raval, Y. Khatavkar and K. Patel, "Patch antenna array using paper as substrate," *International Journal of Microwave and Optical Technology*, vol. 13, no. 1, pp. 26-31, 2018.

[20] S. Kumari and V. R. Gupta, "Measurement of Specific Absorption Rate of Monopole Patch Antenna on human arm," *International Journal of Microwave and Optical Technology*, vol. 10, no. 3, pp. 190-194, 2015.

[21] A. Verma, G. Saini, "Different Size Reduction Techniques of PIFA Antenna: A Review," *ICRTED*, vol. 1 spl issue, pp. 1694-2310, 2014 .

[22] H. T. Chattha, Y. Huang, and Y. Lu, "PIFA Bandwidth Enhancement by Changing the Widths of Feed and Shorting Plates," *IEEE Antennas and Wireless Propagation Letters*, vol. 8, pp. 637-640, 2009.

[23] R. Feick, H. Carrasco, M. Olmos and H.D. Hristov, "PIFA input bandwidth enhancement by changing feed plate silhouette," *Electronics Letters*, vol. 40, no. 15, 2004.

[24] D. B. Lin, I.T. Tang and M. Z. Hong, "A compact Quad Band PIFA by tuning the defected ground structure for mobile phones," *Progress in Electromagnetics Research B*, vol. 24, pp. 173-189, 2010.

[25] F. Afrin , W. A. Yenisey, M. A. A. Syed and R. Farhin, "Design of Slot Loaded Planar Inverted F antenna for Ultra-Wideband Applications," in *IEEE International Conference on Wireless Communications, Signal Processing and Networking (WiSPNET) Conference*, 2017.

[26] K. L. Wong, and C. H. Huang, "Printed PIFA with a coplanar Coupling feed for Penta-band operation in the mobile Phone," *Micowave and Optical Technology Letters*, vol. 50, no. 12, pp. 3181-3186, 2008.

[27] A. Rida, L. Yang, and M. M. Tentzeris, "Design and Characterization of Novel Paper-based Inkjet-Printed UHF Antennas for RFID and Sensing Applications," in *2007 IEEE Antennas and Propagation Society International Symposium*, 2007.

[28] H. P. Phan, T.P. Vuong, P. Benech, P. Xavier, and P. Borel, "Printed Flexible Wideband Microstrip Antenna for Wireless Applications," in *International Conference on Advanced Technologies for Communications (ATC)*, pp. 384-387, 2016.

[29] A. Rida, L. Yang, R. Vyas, S. Bhattacharya and M. M. Tentzeris, "Design and Integration of Inkjet printed Paper-based UHF Components for RFID and Ubiquitous Sensing Applications," in *Proc. of the 37th European Microwave Conference*, Germany, 2007.

[30] S. H. Chang, H. Kuan, H. W. Wu, R. Y. Yang, and M. H. Weng, "Determination of Microwave Dielectric Constant by Two Microstrip Line Method Combined with EM Simulation,"

Microwave and Optical Technology Letters, vol. 48, no. 11, pp. 2199-2201, 2006.

[31] D. C. Thompson, O. Tantot, H. Jallageas, G. E. Ponchak, M. M.Tentzeris and J. Papapolymerou, "Characterization of liquid crystal polymer (LCP) material and transmission lines on LCP substrates from 30 to 110 GHz," *IEEE Transactions on Microwave Theory and Techniques*, vol. 52, no. 4, pp. 1343-1252, 2004.

[32] M. S. Venkatesh and G. S. V. Raghavan, "An overview of dielectric properties measuring techniques," *Canadian Biosystems Engineering*, vol. 47, pp. 7.15-7.30, 2005.

[33] Italian National Research Council, "Calculation of the Dielectric Properties of Body Tissues in the frequency range 10 Hz – 100 GHz". [Online]. Available: http://niremf.ifac.cnr.it/tissprop/htmlclie/htmlclie.php

[34] D.L. Means and K.W. Chan, "Evaluating compliance with FCC guidelines for human exposure to radiofrequency electromagnetic fields," *FCC Supplement C*, ed. 97-01, 2001.

[35] P. McEvoy, M. John, S. Curto and M. Amman, "Group delay performance of ultra wideband monopole antennas for communication applications," in *Antennas and Propagation Conference (LAPC 2008)*, pp. 377-380, Loughborough, 2008.

Sakshi Kumari received her B.Tech degree in Electronics and Communication Engineering from SHUATS, Allahabad in 2007 and M.E in Wireless Communication (ECE) from B.I.T Mesra in 2010. She worked as an Assistant Professor in the department of Electronics and Communication engineering in C.I.T Ranchi, Jharkhand and BITS Edu Campus, Vadodara, Gujarat, India. Currently she is pursuing Ph.D from Birla Institute of Technology Mesra, Ranchi, India. Her publications include seven conference papers and two journal papers. Her research areas are microstrip patch antenna, microwave measurement for material characterization and antenna design using unconventional substrate for body area network applications.

Vibha Rani Gupta received her Bachelor's and Master's degrees in Electronics and Communication Engineering and Ph. D. in Engineering, from Birla Institute of Technology, Mesra, Ranchi, India, in 1986, 1994 and 2007 respectively. Since 2000, she has been working in the Department of Electronics and Communication Engineering, Birla Institute of Technology, Mesra, Ranchi, India. She joined the department as assistant professor and presently working as a professor. She has also served the Department as a Head of the Department from 1st May 2014 to 9th May 2017. Before joining BIT, Mesra, Ranchi, she worked as a lecturer in Department of Science and technology, Bihar, Govt. Women's Polytechnic Ranchi, and Govt. Women's Polytechnic Gorakhpur and as a service cum system engineer M/s Mimec Engineers, Ranchi, India. She is the author of more than 89 technical journal and conference articles. Her current research focuses on surface integrated wave guides, microwave measurement for material characterization, and development of optimized antennas for wearable, medical and wireless applications.